A New Impedance Model for Differentially-fed Proximity-Coupled Microstrip Patch Antennas

Nim R. Ccoillo Ramos, and Jorge L. Salazar-Cerreno
Advanced Radar Research Center (ARRC)
The University *of* Oklahoma, Norman, OK 73019, USA
{nccoillo, salazar}@ou.edu

***Abstract*—This work provides a new analytical model to estimate the impedance response of proximity-coupled microstrip patch antennas excited with a differential feed network. The proposed model has been validated in S- and X-bands. Results show high accuracy estimation of the impedance response over a wide range of frequencies in both bands. This contribution enables analytical modeling of differentially-fed microstrip patch antennas that can be used in radar and communication systems that requires large bandwidth and high polarization purity.**

I. Introduction

Proximity-coupled microstrip patch antennas (PC-MSPAs) [1], [2] have been widely used for a wide range of applications in the last decade [3], [4]. Compared with other conventional feeding techniques, PC-MSPAs provide excellent features for enhancing impedance bandwidth. This is due to the capacitance created by the patch, feed-layer, and ground plane. Adding a differential feed to PC-MSPAs enhances the bandwidth from 1%-5% to 20% [10]. Moreover, if a backed cavity is added to PC-MSPAs, the bandwidth can be increased to 40% [5]. Differentially-feed MSPAs have outstanding stable impedance performance over large frequency operations and offer remarkable performance for high frequencies including millimeter-waves [6], [7].

Previous work has demonstrated that microstrip patch antennas with probe feeding can be modeled as an equivalent electric circuit, showing a high correlation with simulations and measurements in radio-frequency [9]. More recently, an accurate model for single-feeding (SF) PC-MSPA was developed [11]. The feeding was modeled as an inductor and a capacitor in series, all in series with a modified RLC resonator. Moreover, a modeling-based bandwidth estimator [8] proved that SF-PC-MSPA can get impedance bandwidths of up to around 18% in PTFE-like substrates and if using a suitable substrate thickness ratio.

The geometry of a PC-MSPA consists of three conductor layers on two substrates, as shown in Fig. 1. The feed is composed by a transmission line, which partially overlaps the patch in a ratio defined as in (1). Both transmission lines are excited with the same signal amplitude but with a phase difference of 180 degrees, i.e. a differential feeding setup is established in this antenna.

$$x_{0n} = L_0/L \tag{1}$$

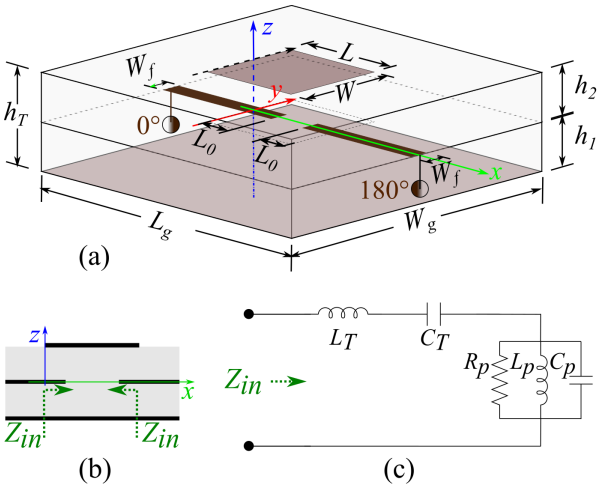

Fig. 1: PC-MSPA with differential feeding: (a) 3D geometry, (b) front view, (c) equivalent circuit

Differential feeding (DF) has the intrinsic feature of broadening bandwidth due to its topology [14]. Mathematically modeling DF-PC-MSPAs in this work will contribute on a novel strategy to evaluate its performance, e.g. an estimation of its impedance behavior. Previous work shows the existence of analytical formulation to model SF-PC-MSPAs [11]. Nonetheless, due to the different field distributions under the patch, as shown in Fig. 2(c)-(d), an inspection of the impedance response of SF-PC-MSPAs and DF-PC-MSPAs is performed.

The impedance behavioral trends of differentially fed PC-MSPAs compared with the one with single feeding can be illustrated in Fig. 2(a)-(b). A PC-MSPA was designed and simulated to show the feeding difference. This antenna consists of two Rogers™5880 substrates ($\varepsilon_r = 2.2, \tan\delta = 0.0009, h = 125$ mil), a square patch of 32 mm, 50-Ω transmission lines, and a square ground plane set to 200 mm each side. Different feeding positions have been included to observe the trends. By comparing the bold and thin lines in Fig. 2(a), it can be noticed that the patch resonant frequency, i.e. the frequency where the maximum of the real part of the impedance occurs, shifts to higher values. Besides, the frequency intervals with the half of the maximum resistance become narrower, i.e. the patch quality factor gets higher. Also, the maximum resistance,

978-1-6654-8609-5/22/$31.00 ©2022 IEEE

which occurs at resonance, increases. Similar trends are seen in the imaginary parts of the antenna impedance.

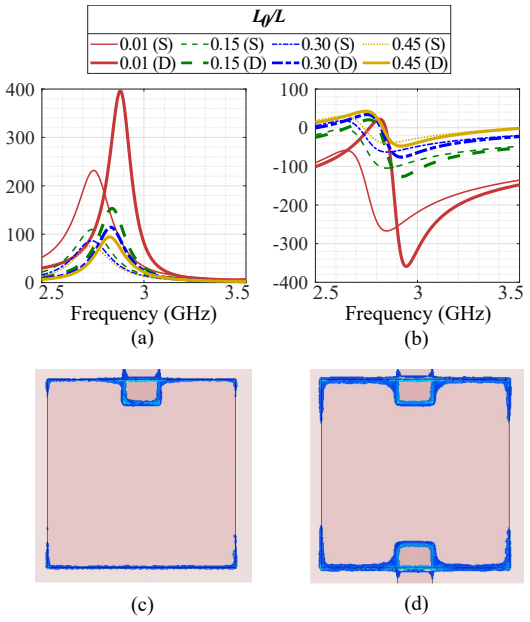

Fig. 2: Variations of impedance response of a PC-MSPA with different feed lengths and feeding setups. (a) Real part. (b) Imaginary part. (c) Fields in SF-PC-MSPA, (d) Fields in DF-PC-MSPA.

Previous analytical model for PC-MSPAs provided in [11] enables a fast analysis of this antenna. Nonetheless, this model can not be used for DF-PC-MSPAs. This work provides an accurate analytical model for the analysis and the design of DF-PC-MSPAs. In the next sections, the proposed model is presented and discussed. Section II delivers the mathematical formulation of the equivalent electric circuit of DF-PC-MSPAs. Section III illustrates the model accuracy by assessing the reflection coefficients between modeled and simulated PC-MSPAs at 3 GHz and 9 GHz. The findings and future work is finally listed in Section IV.

II. Proposed Model

Let be a PC-MSPA comprised by a patch, a transmission line feeding pair, a finite ground plane, all sited on two substrates of relative permittivity ε_r. The two substrates of thicknesses h_1, and h_2 from bottom to top are related by the thickness ratio, as in (2), and add up a total thickness h_T. The ground plane is set to $2\lambda_0$, where λ_0 is the equivalent wavelength of the antenna at its operation frequency. The patch has a length L, and a width W. The feeding transmission lines have dimensions L_f, and W_f, so that the characteristic impedance is set to 50 Ω, and the overlap with the patch is defined through the feed-to-patch ratio, as in (1).

$$R_h = h_2/h_1 \tag{2}$$

The impedance response of a PC-MSPA can be modeled by an equivalent electric circuit composed by a RLC parallel resonator [10], in series with a LC in-series segment [11]. By this means, the patch follows the impedance pattern of the RLC resonator, while the impedance contribution from the feeding comes from the LC segment. This work provides brand-new equations for the shifting factors in the patch resonant frequency and in the patch quality factor, as well as a reformulation of the patch resonant resistance for SF-PC-MSPAs. In the next lines, a set of mathematical equations will be provided, which complete the description of this proposed model.

A. Patch resonant frequency (f_{0p})

Considering that the feeding transmission lines end along the patch length and on the middle of its width, then the dominant propagation mode can be excited for radiation. The resonant frequency of this mode is also the patch resonant frequency, f_{0p}, following the cavity model [9]. Then, for DF-PC-MSPAs, the patch resonant frequency can be calculated as follows:

$$f_{0p} = f_{0r} F_{f0} \frac{f_{0p}^{(D)}}{f_{0p}^{(S)}} = \frac{c_0}{2L_e\sqrt{\varepsilon_{rep}}} F_{f0} \frac{f_{0p}^{(D)}}{f_{0p}^{(S)}}, \tag{3}$$

where $c_0 = 3 \times 10^8$ m/s, L_e and ε_{rep} are defined in [12] and [11], respectively. The factor F_{f0} (4) is defined in [11] as a shifting multiplier from the equivalent resonant frequency of the same patch with a single probe feeding to the one with single proximity-coupled feeding. Furthermore, the factor $f_{0p}^{(D)}/f_{0p}^{(S)}$ introduced in (5) counts the frequency shift of PC-MSPAs due to the differential proximity-coupled feeding, in accordance to the trends observed in Fig. 2. This factor is illustrated in Fig. 3(a).

$$\begin{aligned} F_{f0} = &\left(1.02 - \frac{0.045}{\sqrt{\varepsilon_r}}\right) + \left(\frac{h_T}{\lambda_{0r}} - 0.005\right) \\ &\times \left(\frac{0.7376}{R_h} + 0.4754\right) \frac{1}{\sqrt{\varepsilon_r}} \end{aligned} \tag{4}$$

$$\frac{f_{0p}^{(D)}}{f_{0p}^{(S)}} = 1 + \left(\frac{h_T}{\lambda_{0r}}\right)^2 \left[21.17e^{-0.75R_h} + 4.83e^{-7.3x_{0n}}\right] \tag{5}$$

B. Patch quality factor (Q_p)

The quality factor of the modeled RLC resonator that accounts for the patch (Q_p) [13] comes from the dielectric, the conductor, the radiation, and the surface waves. Thus, Q_p can be computed as in (6).

$$\begin{aligned} Q_p &= [Q_d^{-1} + Q_c^{-1} + (Q_{rad}^{-1} + Q_{sw}^{-1})]^{-1} \\ &= \left[\delta_d + \frac{1}{h_T\sqrt{\pi f_{0p}\mu\sigma}} + \frac{16}{3}\frac{pc_1}{\varepsilon_r}\frac{h_T}{\lambda_{0p}}\frac{W_e}{L_e}\frac{1}{e_r^{hed}}\right]^{-1}, \end{aligned} \tag{6}$$

where δ_d, μ and σ are the substrate loss tangent, the substrate permeability, and the substrate's foil conductivity. The values of p, c_1, and e_r^{hed} are defined with more detail in [13].

Since Q_{rad}, the portion of Q_p that comes from radiation, generally possesses the lowest value among the other values

(Q_d, Q_c, Q_{sw}), a reformulation has been performed to provide more accuracy. This reformulation has been done by comparing the quality factors from the real part of impedance responses of SF-PC-MSPAs with loseless materials, so that $Q_p = (Q_{rad}^{-1} + Q_{sw}^{-1})^{-1}$. Then, Q_p can be rewritten for DF-PC-MSPAs as:

$$Q_p = \frac{1}{\delta_d + \frac{1}{h_T\sqrt{\pi f_{0p}\mu\sigma}} + \frac{Q_{rp}^{(S)}}{Q_{rp}^{(D)}} {R_h}^{0.24} \frac{16}{3} \frac{pc_1}{\varepsilon_r} \frac{h_T}{\lambda_{0p}} \frac{W}{L} \frac{1}{e_r^{hed}}}, \quad (7)$$

where the factor ${R_h}^{0.24}$ multiplies the inverse of the radiation quality factor Q_{rad}^{-1}, and counts for the influence of the substrate thickness ratio in PC-MSPAs. Besides, the factor $Q_{rp}^{(D)}/Q_{rp}^{(S)}$ (8) multiplies Q_{rad} when the PC-MSPA presents a differential feeding setup. A numeric example of this factor is pictured in Fig. 3(b).

$$\begin{aligned} \frac{Q_{rp}^{(D)}}{Q_{rp}^{(S)}} = 1 + \frac{1}{100}\Bigg[& 4.32 \frac{e^{36h_T/\lambda_{0r}}}{{R_h}^{1.25}} \Big(\frac{L}{W}\Big) \\ & + 1.54 \frac{e^{60h_T/\lambda_{0r}}}{R_h} \left(\frac{25L}{44W} + \frac{19}{44}\right) e^{-10x_{0n}} \Bigg] \end{aligned} \quad (8)$$

C. Patch resonant resistance (R_p)

The resonant resistance in PC-MSPAs can be written as:

$$R_{pM} = \frac{4}{\pi}(\mu_r\eta_0) Q_p \Big(\frac{h_T}{\lambda_{0p}}\Big) K_R \quad (9)$$

$$R_p = R_{pM} F_{Rp} \quad (10)$$

In this work, the expression of R_p is revised and reformulated, including variations on the relative permittivity. Then:

$$K_R = 1.1\varepsilon_r^{-0.02\lambda_{0p}/h_T} \Big(\frac{W}{L}\Big)^{0.75} {R_h}^{-0.8+4.44\sqrt{h_T/(\varepsilon_r\lambda_{0p})}} \quad (11)$$

$$F_{Rp} = Ae^{-p_1 x_{0n}} + (1-A)e^{-p_2 x_{0n}}, \quad (12)$$

where

$$\begin{aligned} A = {} & 0.58 - 1.8e^{-270\frac{h_T}{\lambda_{0r}}\frac{1}{\varepsilon_r}} \\ & + (\ln R_h)\Big[0.1732 + 130.8\Big(\frac{h_T}{\lambda_{0r}}\frac{1}{\varepsilon_r} - 0.03135\Big)^2\Big] \end{aligned} \quad (13)$$

$$p_1 = \frac{2}{\frac{h_T}{\lambda_{0r}}\sqrt{\varepsilon_r} + 0.035} \quad (14)$$

$$p_2 = 1.35 R_h^{0.75}\Big[1 - 1.25e^{-50\frac{h_T}{\lambda_{0r}}\varepsilon_r^{-0.63}}\Big] \quad (15)$$

This formulation has been performed through the curve fitting technique [15], after obtaining, analyzing, and mathematically describing the impedance responses in several PC-MSPAs. The variations made included total thicknesses (from 31.25 mil to 250 mil at 3 GHz), patch length over width ratio (0.75 to 1.25), relative permittivity (1.1, 2.2, and 4.4), and substrate thickness ratio (from 0.67 to 1.50).

D. Feeding circuit (L_T, C_T)

The impact of the feeding on the impedance response of PC-MSPAs can be evaluated by the reactances produced by an inductor and a capacitor connected in series. Let be the feeding inductor named L_T, and the feeding capacitor, C_T. Then, the values of L_T, C_T are expressed as [11]:

$$L_T = \frac{0.4674}{f_{0p}\sqrt{\mu_r}} e^{4.551 x_{0n}} \quad (16)$$

$$C_T = \frac{1}{f_{0p}\sqrt{\varepsilon_r}}\big[-48.05(x_{0n} - 0.4534)^2 + 7.85\big], \quad (17)$$

where f_{0p} is expressed in GHz, L_T is given in nH, and C_T is specified in pF.

E. Impedance response

For SF-PC-MSPAs [11], the input impedance at the origin of the overlap between the patch and the feed can be written as:

$$Z_{11} = Z_p + Z_f \quad (18)$$

$$= \frac{1}{1/R_p + 1/j\omega L_p + j\omega C_p} + \Big(j\omega L_T + \frac{1}{j\omega C_T}\Big), \quad (19)$$

where Z_p and Z_f are the impedances of the patch resonator, and of the feed, respectively. Also, the values of L_p, and C_p can be obtained by replacing the values from (3), (7), and (10) in the expressions (20)-(21):

$$L_p = \frac{R_p}{2\pi f_{0p} Q_p} \quad (20)$$

$$C_p = \frac{Q_p}{2\pi f_{0p} R_p} \quad (21)$$

From the theory of differential feeding setup [16], [17], the assessment of these antennas is made through the differential input impedance Z_{11d}. Let be the ports named "1" and "2", one in front of the other one along the PC-MSPA, and configuring differential feed. Then, the impedance parameters generated in this bi-port network are: Z_{11}, Z_{12}, Z_{21}, and Z_{22}. In each port there is one self impedance (Z_{11}, Z_{22}), and one mutual impedance (Z_{12}, Z_{21}).

For symmetrically-fed microstrip antennas:

$$Z_{11} = Z_p + Z_f \quad (22)$$

$$Z_{12} = -Z_p \quad (23)$$

$$Z_{21} = -Z_p \quad (24)$$

$$Z_{22} = Z_p + Z_f, \quad (25)$$

Then, applying the definition of differential input impedance Z_{11d} [17], and considering symmetrically feeding:

$$\begin{aligned} Z_{11d} &= Z_{11} - Z_{21} - Z_{12} + Z_{22} \\ &= 2(Z_p + Z_f) - 2(-Z_p) \\ &= 4Z_p + 2Z_f \end{aligned} \quad (26)$$

Thus, the impedance response of a DF-PC-MSPA can be evaluated by the expression derived in (26). Furthermore,

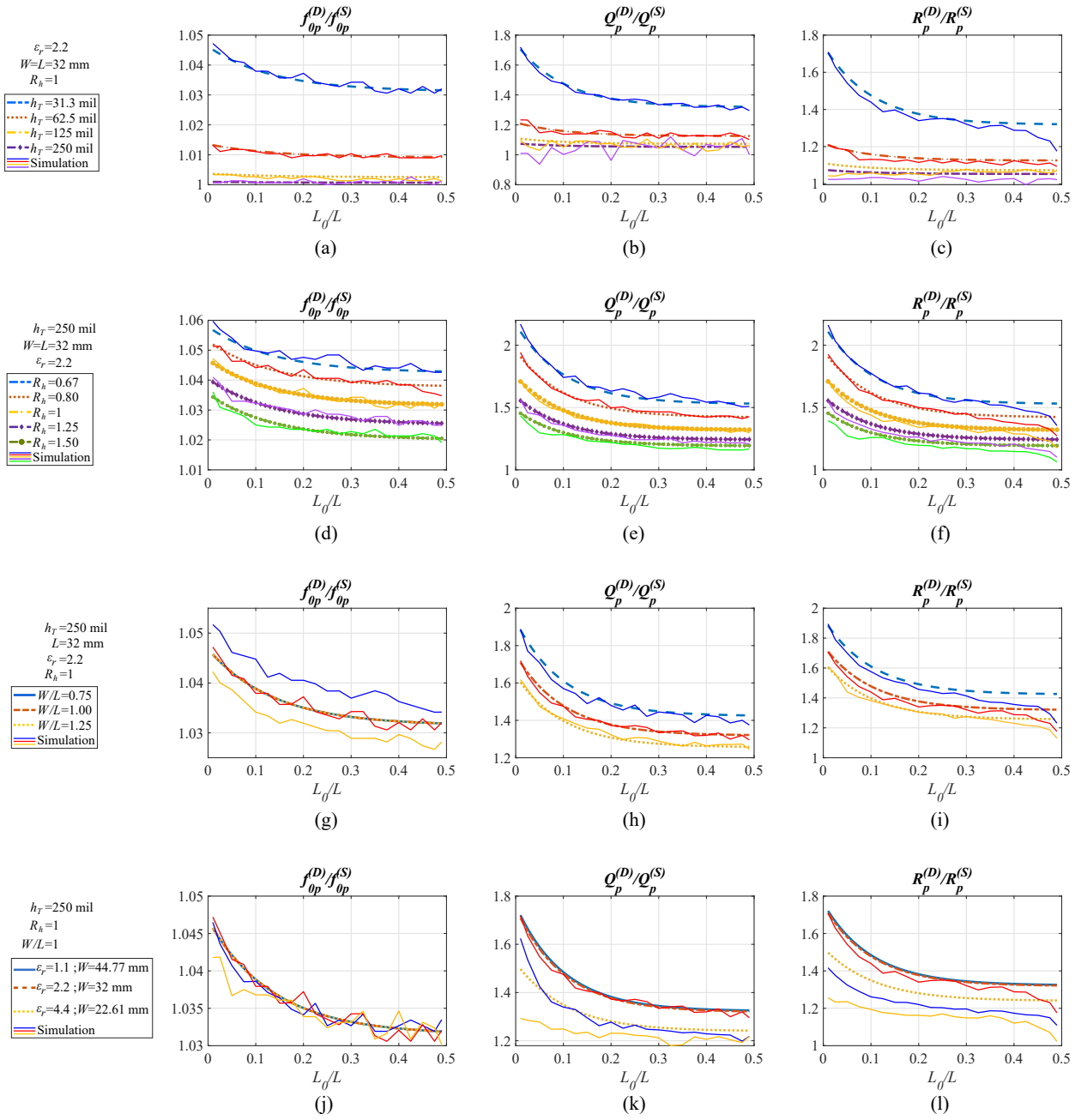

Fig. 3: Comparison of modeled and simulated ratios between patch RLC parameters for DF-PC-MSPA and SF-PC-MSPA: First column: Patch resonant frequency (f_{0p}), Second column: Quality factor (Q_p), Third column: Resonant resistance (R_p).

previous work already has demonstrated that the contribution of a patch in differential feeding gets multiplied by four [17], which is noticed in the first term of (26).

III. Assessment

To assess the formulations made in this work, different variations have been made. In Fig. 3, the proposed shifting factors of (5) and (8) are evaluated and compared with the observed shifting factors from simulated antenna variations in total thickness, substrate thickness ratio, patch size ratio, and permittivity. Also, the differential impedance of two antennas in S and X band is evaluated to assess the accuracy of the impedance model. The antenna specifications are listed in Table I, and the impedance responses are pictured in Fig. 4.

The plots in Fig. 3 suggest that the proposed shifting factors $f_{0p}^{(D)}/f_{0p}^{(S)}$ and $Q_{rp}^{(D)}/Q_{rp}^{(S)}$ follow accurately the observed shifts in DF-PC-MSPAs. As shown in the first row of Fig. 3, the proposed model allows the prediction the impact of the differential feeding in PC-MSPAs in a wide range of thickness, from $0.008\lambda_0$ (31.25 mil at 3 GHz) to $0.064\lambda_0$ (250 mil at 3 GHz). Moreover, the proposed model follows the perceived variations in the RLC parameters when the substrate thickness

TABLE I: Assessed antennas' specifications.

Specifications		Units	Design 1	Design 2
Relative permittivity	ε_r	-	2.2	2.2
Loss tangent	h_a	mm	0.0009	0.0009
Patch size	L, W	mm	24.2	8
Total substrate thickness	h_T	mm	3.175	1.575
Substrate thickness ratio	R_h	mm	1.00	1.00
Feed-to-patch overlap ratio	x_{0n}	-	0.125	0.125
Cell size	L_g	mm	200	50

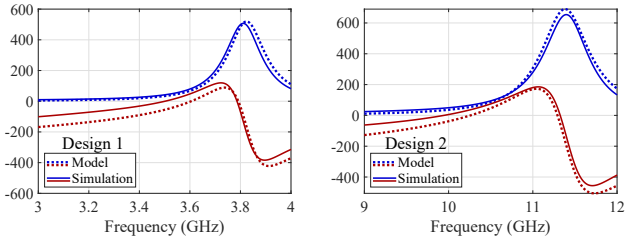

(a) (b)

Fig. 4: Comparison between modeled and simulated impedance responses for PC-MSPAs in S and X bands.

ratio varies, as noticed in the second row of Fig. 3. This is an important finding since the main variable that affects the performance of PC-MSPAs is this substrate ratio, which even sets the limits of maximum bandwidth that it can get, as found in [8]. The third row of Fig. 3 illustrates the accuracy of the proposed model on following the shifts in the patch resonator parameters. Despite that the model does not include a variation in patch length over width ratio, it does not produce deviations more than 0.5% in the estimation. Furthermore, it is observed that the proposed model can follow accurately the variations in the patch resonant frequency. It is also observed that the proposed model works best with dielectric constant around 2.2, as suggested in the plots (k) and (l). This optimization is advantageous since many broadband antennas are developed with materials with similar dielectric constants.

Fig. 4 shows that the model accurately predicts the impedance response in S-band and X-band antennas. The real part is followed almost completely, while the imaginary part has some slight variations outside the resonance. These results suggest that the proposed shifting factors work very well and get accurate RLC resonators. They also suggest that the proposed work can be enhanced by including a further analysis of the impact of the differential feeding on the LC-series feed.

IV. Conclusion

The equivalent electrical circuit of a PC-MSPA can still be modeled as an RLC parallel circuit in series with a LC series circuit. However, this circuit model required additional reformulation to be accurate for DF-PC-MSPAs. The proposed model enables an estimation of the differential impedance response of DF-PC-MSPAs proving an accuracy less than 1% in the patch resonance frequency. Also, the shifting factors in the patch quality factor and resonant resistance show a very good agreement between model and simulation. Finally, the validations in the S and X bands showed a high accuracy in the estimation of the impedance response of DF-PC-MSPAs.

Acknowledgment

The authors thank the Advanced Radar Research Center of The University of Oklahoma, and to the Phased Array Antenna Research and Development group for the facilities and feedback received in this research. This research was partially sponsored by the U.S. Dept. of Commerce, National Oceanic.

References

[1] D. M. Pozar and B. Kaufman, "Increasing the Bandwidth of a Microstrip Antenna by Proximity Coupling," Electronics letters, vol. 23, no. 8, pp. 368–369, 1987.

[2] P. Bhartia, I. Bahl, R. Garg, and A. Ittipiboon, *Microstrip Antenna Design Handbook*, Artech House, London, 2001.

[3] M. K. M. Amin, M. F. Mansor, N. Misran and M. T. Islam, "28/38GHz Dual Band Slotted Patch Antenna with Proximity-Coupled Feed for 5G Communication," 2017 International Symposium on Antennas and Propagation (ISAP), 2017, pp. 1-2, doi: 10.1109/ISANP.2017.8228897.

[4] A. K. Awasthi et al., "Ultra-Wideband Patch Antenna Array With an Inclined Proximity Coupled Feed for Small Unmanned Aircraft RADAR Applications," in IEEE Open Journal of Antennas and Propagation, vol. 2, pp. 1079-1086, 2021, doi: 10.1109/OJAP.2021.3128015.

[5] D. Sun, Z. Zhang and X. Yan, "A Wideband Dual-polarized Patch Antenna," Proceedings of 2014 3rd Asia-Pacific Conference on Antennas and Propagation, Harbin, pp. 84-86, 2014.

[6] G. Varshney, A. Verma, V. S. Pandey, R. S. Yaduvanshi, and R. Bala, "A Proximity Coupled Wideband Graphene Antenna with the Generation of Higher Order TM Modes for THz Applications," Optical Materials, vol. 85, pp. 456–463, 11 2018

[7] M. A. Jamshed, A. Nauman, M. A. B. Abbasi, and S. W. Kim, "Antenna Selection and Designing for THz Applications: Suitability and Performance Evaluation: A Survey," IEEE Access, vol. 8, pp. 113246-113261, 2020.

[8] N. Aboserwal, N. R. Ccoillo Ramos, Z. Qamar, and J. L. Salazar-Cerreno, "An Accurate Analytical Model to Calculate the Impedance Bandwidth of a Proximity Coupled Microstrip Patch Antenna (PC-MSPA)," IEEE Access, vol. 8, pp. 41784-41793, 2020.

[9] K. Carver and J. Mink, "Microstrip Antenna Technology," in IEEE Transactions on Antennas and Propagation, vol. 29, no. 1, pp. 2-24, 1981.

[10] C. Balanis, *Antenna Theory : Analysis and Design, 4th ed.*, John Wiley Sons, 2015.

[11] N. R. Ccoillo-Ramos, N. Aboserwal, J. Salazar-Cerreno, and Z. Qamar, "Improved Analytical Model for a Proximity Coupled Microstrip Patch Antenna (PC-MSPA)," IEEE Transactions on Antennas and Propagation, 2021.

[12] M. Kirschning, R. H. Jansen, and N. H. L. Koster, "Accurate Model for Open End Effect of Microstrip Lines," Electronics Letters, vol. 17, no. 3, pp. 123-125, 1981.

[13] D. R. Jackson, S. A. Long, J. T. Williams, and V. B. Davis, "Computer-Aided Design of Rectangular Microstrip Antennas," in Advances in Microstrip and Printed Antennas. Wiley Series in Microwave and Optical Engineering, W. C. K. F. Lee, Ed. New York, NY, USA: John Wiley ans Sons Inc., 1997, ch. 5, pp. 223–272.

[14] S. V. Hum and H. Y. Xiong, "Analysis and Design of a Differentially-Fed Frequency Agile Microstrip Patch Antenna," in IEEE Transactions on Antennas and Propagation, vol. 58, no. 10, pp. 3122-3130, Oct. 2010, doi: 10.1109/TAP.2010.2055805.

[15] S. L. Arlinghaus, *Practical Handbook of Curve Fitting*. CRC Press, 1994

[16] Y. P. Zhang and J. J. Wang, "Theory and Analysis of Differentially-driven Microstrip Antennas," in IEEE Transactions on Antennas and Propagation, vol. 54, no. 4, pp. 1092-1099, April 2006, doi: 10.1109/TAP.2006.872597.

[17] Z. Tong, A. Stelzer and W. Menzel, "Improved Expressions for Calculating the Impedance of Differential Feed Rectangular Microstrip Patch Antennas," in IEEE Microwave and Wireless Components Letters, vol. 22, no. 9, pp. 441-443, Sept. 2012, doi: 10.1109/LMWC.2012.2212240.